N88-23098

Center for Turbulence Research
Proceedings of the Summer Program 1987

Premixed turbulent flame calculation

By S. EL-TAHRY[1], C. J. RUTLAND[2], J. H. FERZIGER[2] AND M. M. ROGERS[3]

The importance of turbulent premixed flames in a variety of applications has led to a substantial amount of effort towards improving our understanding of these flames. Although these efforts have increased our understanding, many questions remain. For example, there is contradicting evidence concerning the role of the turbulent length scales on turbulent flame speed. There are a variety of proposals that attempt to correlate the turbulent flame speed with the turbulence velocity (*e.g.*, Bray, 1980 and zur Loye and Bracco, 1987). As in non-reacting turbulent flows, the main impediment is the inability to both adequately control experiments and to adequately measure the quantities of interest in the experiments. With recent advances in supercomputers and the accompanied development of direct numerical simulation (DNS) it might now be possible to alleviate some of these difficulties.

There are a variety of questions that are currently being raised in turbulence combustion modeling work for which DNS can provide answers. For example, what is the instantaneous structure of a premixed turbulent flame? Flame structures are difficult to obtain experimentally because of the fine resolution required. Knowledge of the flame structure can aid in closing the viscous dissipation term in the equation for the variance of relevant scalars (for a related example see Pope and Anand, 1985). It is anticipated that in the thin flame mode of combustion (*i.e.*, when the turbulence strain rate is small compared to the reciprocal of the chemical time scale), the flame structure is similar to an undisturbed laminar flame. We need to test this assumption under a variety of circumstances such as different chemical systems, different Lewis numbers, and different ratios of turbulent velocity to laminar flame speeds (u'/S_L).

A fundamental question that can be addressed with DNS is what factors control the turbulent flame speed (S_T). For example, what are the turbulence characteristics that control S_T and what is the form of the correlation of these characteristics? In DNS we know the values of all quantities at each grid point at every time step. In addition, both Eulerian and Lagrangian (*i.e.*, following the flame surface) analyses can be conducted and parameters can be switched on and off. Thus with DNS more information can be gained than is possible experimentally and many questions can be addressed. However, there are limitations to DNS and these are reviewed next.

The first limitation of all DNS is the range of scales which can be resolved. Small grid spacing is required to resolve small scales and large domain size is needed to capture the large scales. Computer resources limit this range and hence limit

1 General Motors Research Laboratory
2 Dept. of Mech. Engng., Stanford University
3 NASA-Ames Research Center

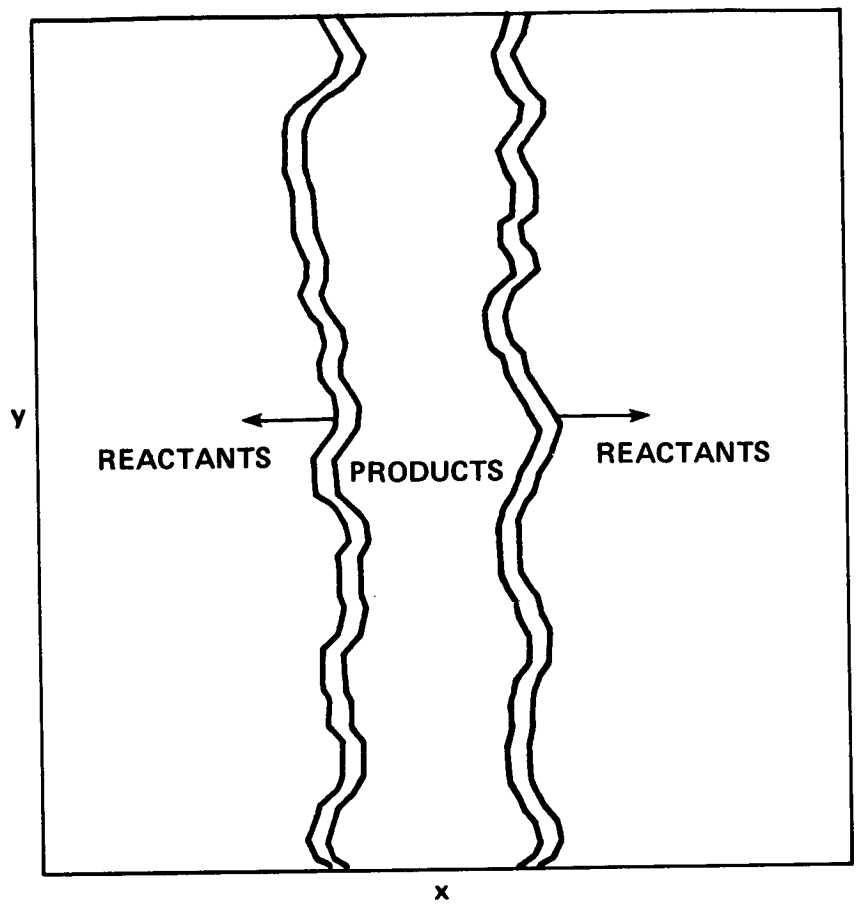

FIGURE 1. Schematic of the flame geometry.

the maximum Reynolds number of the computations. In the presence of premixed flames there is a more stringent condition on the Reynolds number that arises if calculations are to be made in the more interesting thin flame regime that occurs at high Damkohler numbers (Da). We define Da based on the strain rate of the turbulence *i.e.*,

$$Da = \frac{\lambda S_T}{\delta u'} ,$$

where λ and δ are the Taylor microscale and the flame thickness, respectively. Then, it is generally accepted that the thin flame regime is achieved with Da greater than unity. To reveal the extra constraint on the Reynolds number in the thin flame regime, we can rewrite Da as

$$Da = \left(N_1 Re_L^{-0.75}/N_2 n\right)^2 , \tag{1}$$

where N_1 is the number of grid lines spanning the computational domain along a coordinate direction, N_2 is the number of grid points that will span the flame

thickness, Re_L is the Reynolds number based on the integral length scale and n is the number of integral length scales present in the computational domain.

In deriving (1) we used the standard relations between the turbulent scales, hence the equation is to be used only for order-of-magnitude purposes, particularly at small Reynolds numbers. We notice that N_1 is constrained by the maximum job size that can be run and N_2 is limited by resolution considerations. We cannot set n too low; otherwise the large eddies become too large for the computational domain before there has been sufficient time for the flame to develop and propagate. Thus, the only avenue available to obtain large Damkohler numbers is to reduce Re_L.

The other relevant constraints on the DNS calculations are the periodic boundary conditions and the limitation to incompressible flows. These constraints are particular to the computer code that is used in the present study (Rogallo, 1981) and in principle can be eliminated. The former constraint may not be too significant. The latter constraint, however, precludes studying important aspects, such as the influence of the flame on the turbulence and the effect of hydrodynamic flame instabilities on the flame structure. The present work is an initial effort in studying thin premixed flames using DNS. We attempt to address some of the questions raised earlier and we do so under the mentioned constraints.

The problem considered is shown schematically in Figure 1. It consists of a planar flame sheet, located in the y-z plane, initiated at the midpoint of the x-direction. The chemical kinetics model used is a hypothetical, single-step kinetics with a single reactant A going to a product B. The equations which govern the thermal and chemical states are the conservation equations for species A mass fraction, Y_A, and the temperature, T. These are:

$$\frac{DY_A}{Dt} = \gamma_Y \nabla^2 Y_A - bY_A \exp(-T_a/T) \tag{2}$$

$$\frac{DT}{Dt} = \gamma_T \nabla^2 T - bHY_A \exp(-T_a/T)\,, \tag{3}$$

where D/Dt is the substantial derivative, γ_Y and γ_T are the (uniform and constant) diffusivities of mass and heat, respectively, b is a pre-exponential factor, T_a is the activation temperature, and H is the enthalpy of the reaction. In the present calculation we have taken the diffusivities of mass and heat to be equal (*i.e.*, the Lewis number is unity). For Lewis number not equal to unity, a term involving species diffusion should be added to the temperature equation. The value of H was selected so as to yield a temperature rise of 15° across the flame. This ensured a small density variation due to the reaction so that our assumption of a divergence-free velocity field is acceptable. The values of b and T_a were selected to give a flame thickness spanning about 10 grid lines and an inner flame region spanning about 4 grid lines. The values of these quantities were established by trial and error using a laminar flame code.

To implement (2) and (3) in the DNS code (Rogallo, 1981), the source terms had to be added to the already existing scalar equations and a chemical time step

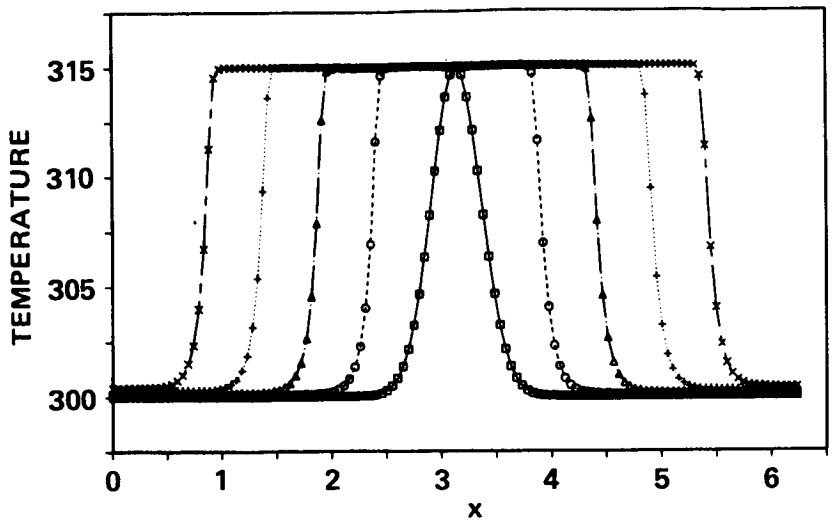

FIGURE 2. Laminar temperature profiles at 400 step intervals.

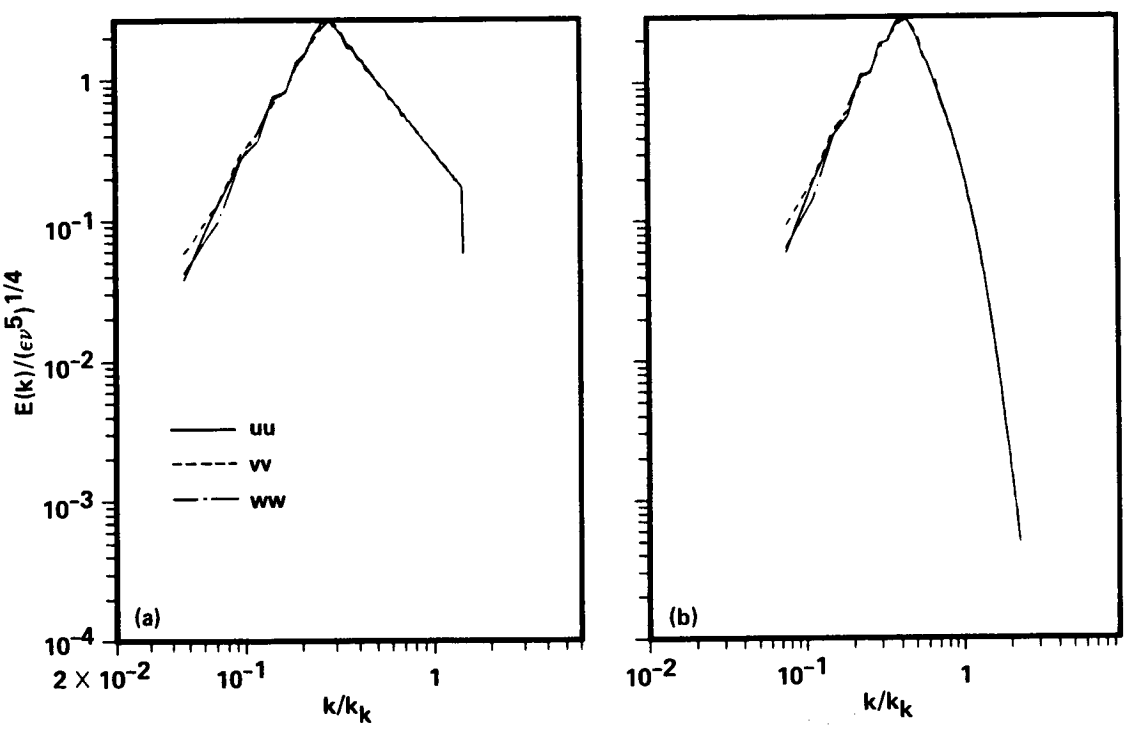

FIGURE 3. Velocity energy spectra (a) Initial spectra (b) Spectra after 50 steps, at the beginning of the reacting part of the calculation.

stability constraint had to be implemented. The calculations were performed with a $128 \times 128 \times 128$ grid.

To test the accuracy of the flame calculation with the DNS code, a laminar flame

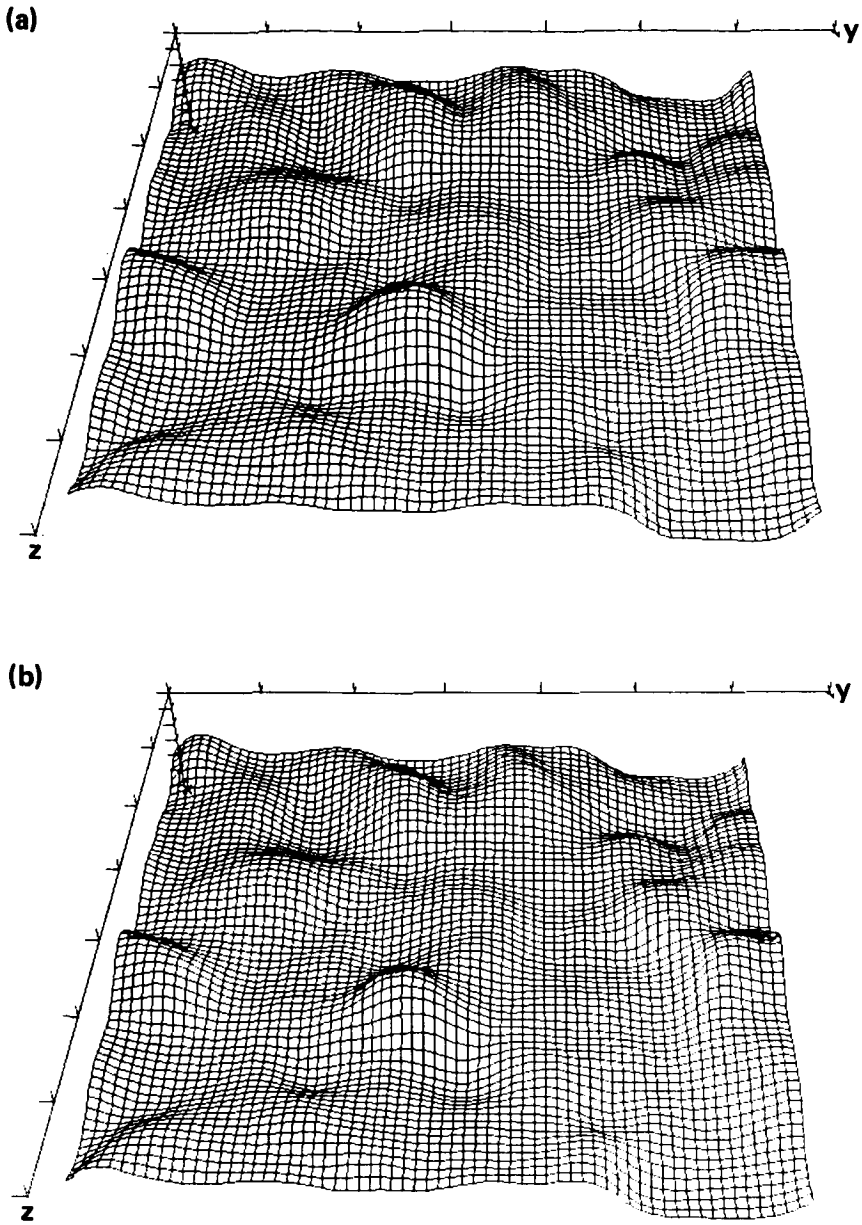

FIGURE 4. Constant temperature surfaces (a) $T = 302°$ (b) $T = 314°$.

propagation calculation was made on the same geometry as depicted in Figure 1 and the results were compared to the results of a similar calculation made with an accurate laminar flame code. The results of the laminar flame calculations made with the DNS code are shown in Figure 2. The figure shows the temperature profiles at 400 step intervals which begin at $t = 0$ with a Gaussian distribution. It is seen that after 400 time steps the profile has significantly steepened relative to the initial conditions and the flame thickness has approximately stabilized (*i.e.*, the initial conditions are forgotten). Comparison of the flame speeds obtained from the two

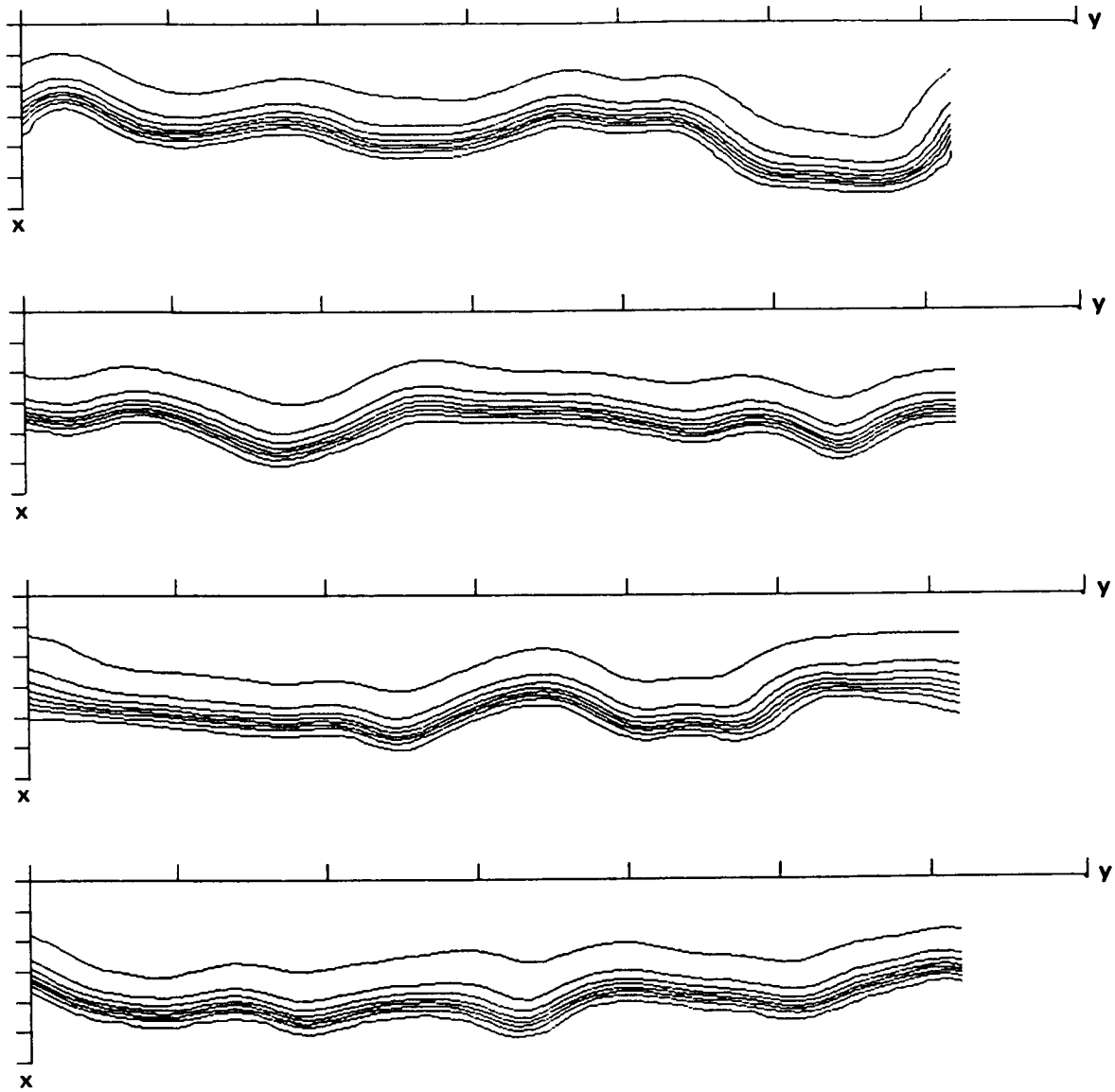

FIGURE 5. Temperature contours in x-y planes (a) z station = 0 (b) z station = 1/4 (c) z station = 1/2 (c) z station = 3/4.

codes were found to be within 2% of each other. This is good agreement considering that only about 10 grid points were within the flame and that no de-aliasing was attempted for the non-linear source terms.

For the turbulent combustion calculations, the underlying hydrodynamic field was an unforced isotropic turbulence. To achieve a developed turbulence spectrum at the start of the chemistry calculations, the latter calculations were initiated after developing the hydrodynamics field for 50 time steps. The turbulence spectrum at $t = 0$ and after 50 time steps are shown in Figure 3. The Reynolds number based

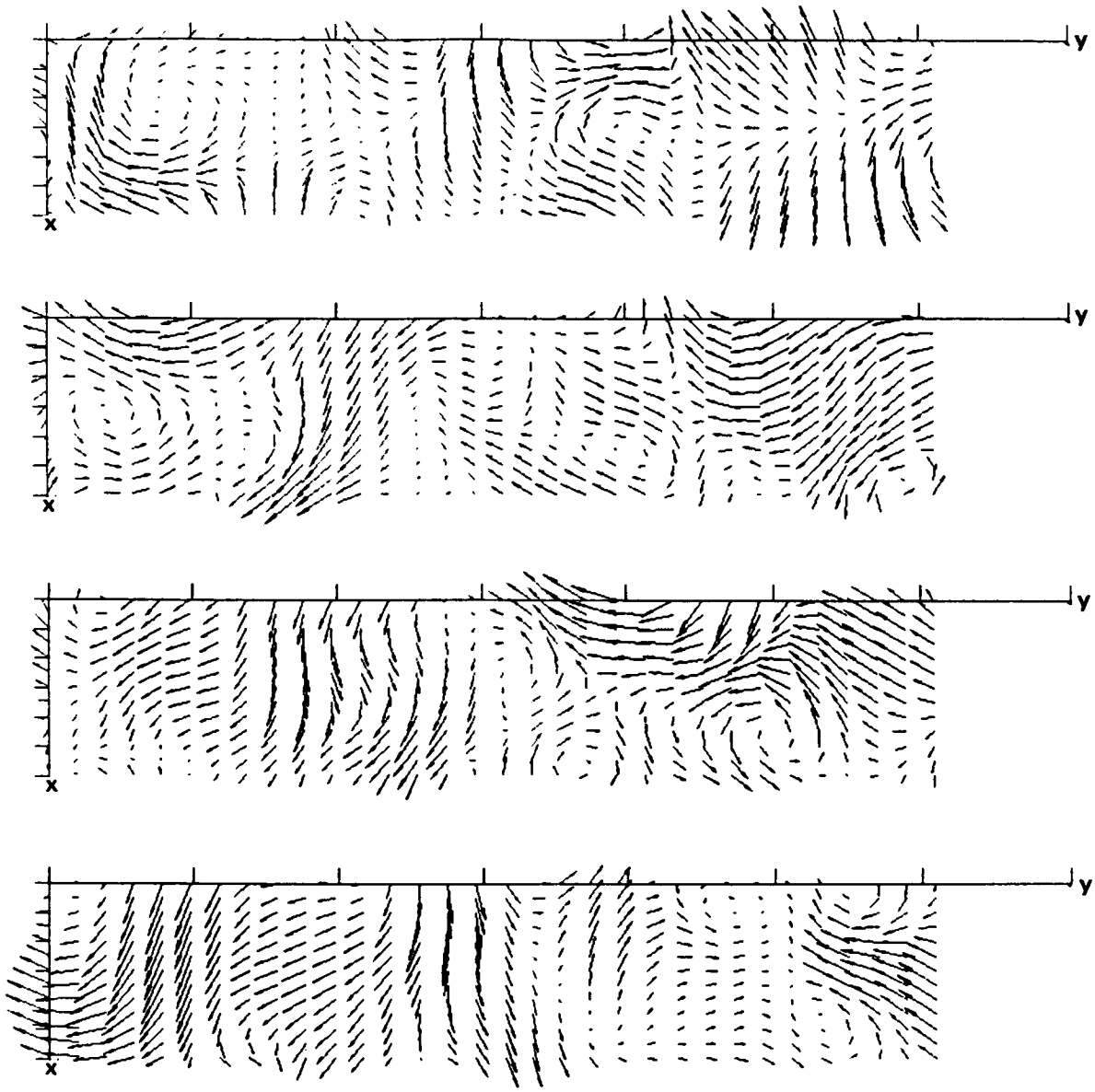

FIGURE 6. Velocity vectors in x-y planes (a) z station = 0 (b) z station = 1/4 (c) z station = 1/2 (c) z station = 3/4.

on the Taylor microscale was approximately 5, Da was approximately equal to 1.5 and u'/S_L was of the order 0.53. This meant that we expect a thin flame with low turbulence (*i.e.*, the wrinkled flame regime).

We start reviewing the results by examining the flame structure. Figure 4 shows the constant temperature surfaces for $T = 302°$ and $T = 314°$ (the unburned temperature is 300° and the burned temperature is 315°). The surfaces are seen to have a wavy topology consistent with what is expected in the wrinkled flame regime. Figure 5 shows contours of constant temperatures in x-y planes taken at

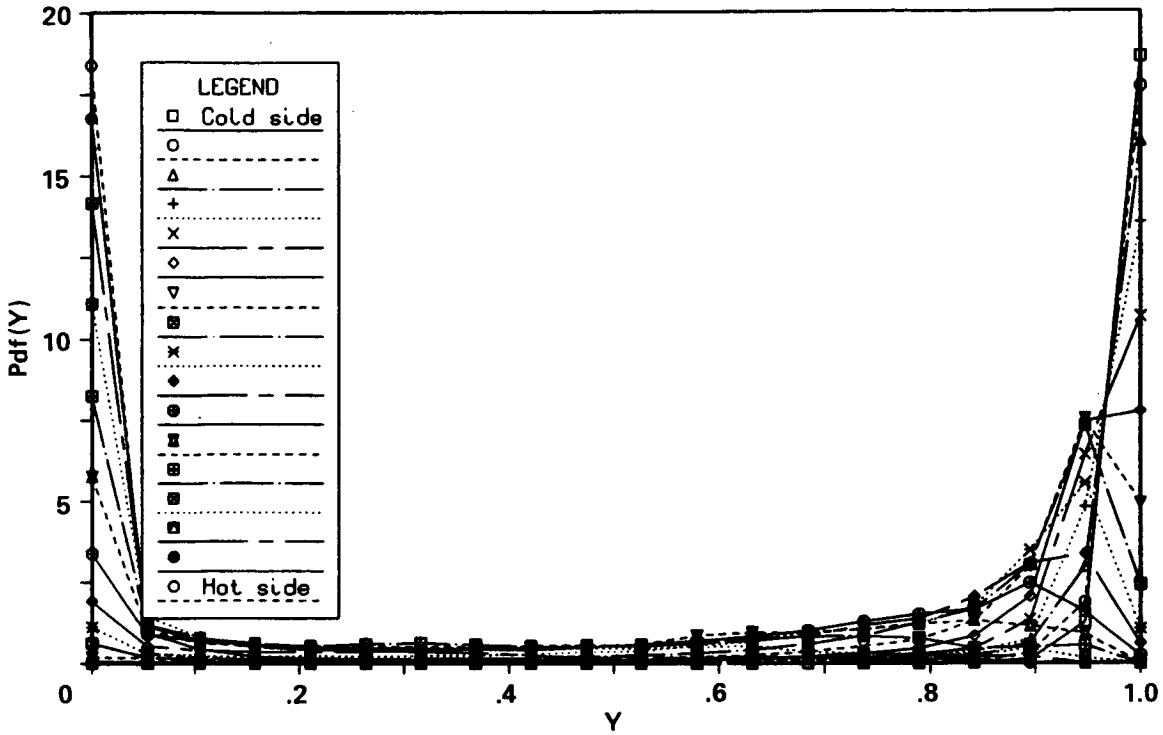

FIGURE 7. PDF of the mean reactant mass fraction.

the 0, 1/4, 1/2, and 3/4 stations in the z-direction. Here the wrinkled structure is more evident and the wrinkling seems to be occurring at several scales. The flame thickness is found to vary with location. This variation is caused by the inclination of the local flame front relative to the section plane. Thus the flame appears thicker than it is along a normal to the flame front. The flame thickness in the thin regions were found to be comparable to the thickness of the laminar flame calculated earlier. At thirteen locations tested the flame structure was also found to be similar to the laminar flame structure. This result agrees with the first-order solution derived by Clavin and Williams (1979). However, their second-order solution modifies the laminar profile.

Figure 6 shows the velocity vector field in x-y planes at the same z-locations as Figure 5. In these figures the flame wrinkling appears for the most part to follow the velocity field. We can also see that on the scale of the flame thickness the strain rate is small. This qualitatively verifies that we are in the thin flame regime.

The probability density function (PDF) for the reactant mass fraction is shown in Figure 7 at various x-locations. These PDFs were generated by collecting data from the homogeneous planes (y-z planes) at the specified x locations, dividing it into 20 bins and averaging the data in each bin. The distributions are seen to be qualitatively similar to the PDF of the laminar flamelet model proposed by Bray and Moss (1977). According to this model the PDF consists of two delta functions located at $Y_A = 0$ and $Y_A = 1$ which are joined by a region of low probability

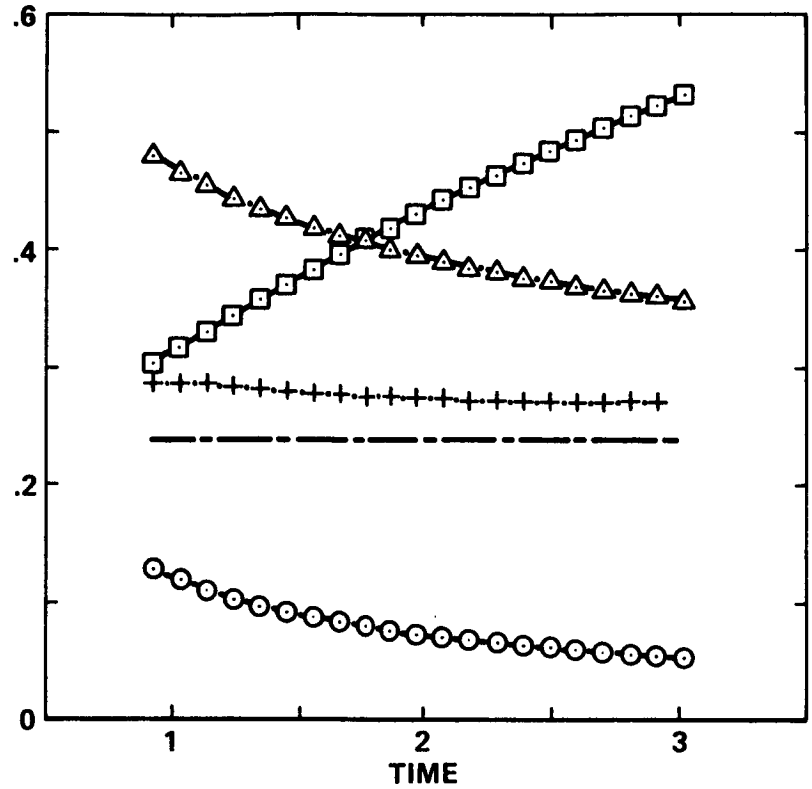

FIGURE 8. Various scales and velocities as a function of time. □ Taylor microscale; ○ u'; △ Reynolds number/10; + Turbulent flame speed; — - — Laminar flame speed.

that has its PDF proportional to the inverse of the gradient of Y_A. We notice from Figure 7 that, because the gradients on the cool side of the flame are small, the probability density function tends to be higher at the large values of Y_A. There is, however, a peculiar behavior of the PDFs at some of the x-locations where we observe a maximum of the PDF at values of Y_A of around 0.9. This probably indicates that the wrinkling of the flame is not much larger than the flame thickness. This is supported by the contour plots in Figure 5.

Next we will examine the dependence of the turbulent flame speed on u'. Figure 8 depicts the variation of λ,u', Re_λ and the turbulent flame speed S_T with time. The laminar flame speed is also included for comparison. The hydrodynamic quantities display the expected behavior *i.e.*, u' and Re_λ decrease with time, while λ increases. Hence, Da will increase with time which means that we remain in the wrinkled flame regime for the duration of the calculation. The variation of the turbulent flame speed with u' is shown in Figure 9. We find S_T increasing with u' but the increase is much slower than suggested by the commonly used formula

$$S_T = S_L + c'u' \,, \tag{4}$$

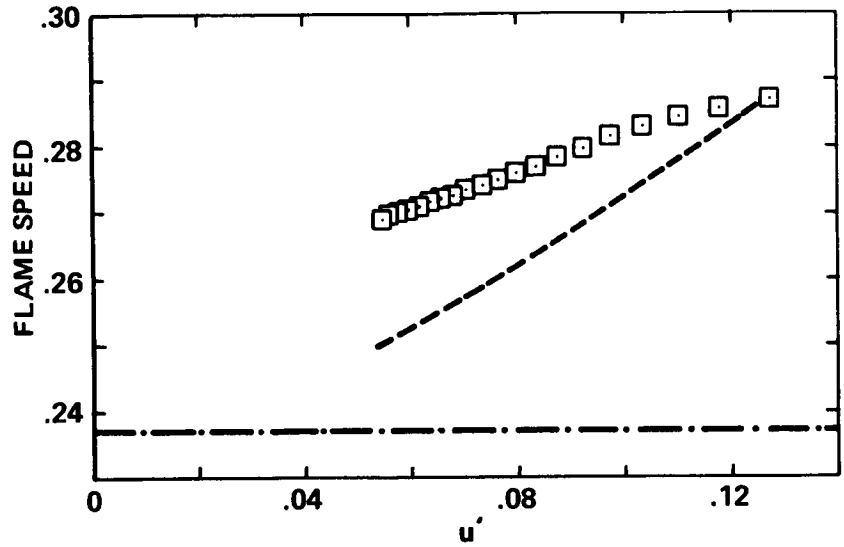

FIGURE 9. Flame speed vs. u'. □ Turbulent flame speed; - - - - Williams' equation; — · — Laminar flame speed.

where c' is a constant. Tabaczyski *et al.* (1974) use $c' = 1$, Witze and Mendes-Lopez (1986) suggest a value of 2.2. For other suggestions see zur Loye and Bracco (1987). Our results are closer to the theoretically obtained formula given by Clavin and Williams (see Williams 1985) for weak turbulence

$$S_T = S_L \left[\frac{1}{2} \left(1 + \sqrt{1 + 8c(u'/S_L)^2} \right) \right]^{1/2} , \tag{5}$$

where c is a constant of order unity. This equation is also plotted in Figure 9 using $c = 1.2$ to match the first data point. Within the range of our data the magnitude of S_T/S_L given by equation (5) is fairly close to our calculated values. However, the trend is not, indicating that S_T probably depends on more than just u'. It is interesting to note that in equations (4) and (5) and most other suggestions in the literature, there is no dependence of S_T/S_L on heat release or Reynolds number (there are some exceptions *e.g.*, Abdel-Gayad and Bradley (1976) give an expression that involves the Reynolds number). Hence the flame speeds calculated with the DNS code should also be representative of flames with large density variation and large Reynolds numbers. However, as implied earlier, the differences in the various proposed equations for the flame speed may be due to not including all of the relevant parameters on which the flame speed depends. We should try to investigate these systematically.

Finally, the development of the mean temperature profiles is shown in Figure 10. The profiles suggest that the turbulent flame thickness is about twice the laminar flame thickness. We also observe that the flame thickness increases with flame travel. This may be due to the increase of the turbulent length scale with time.

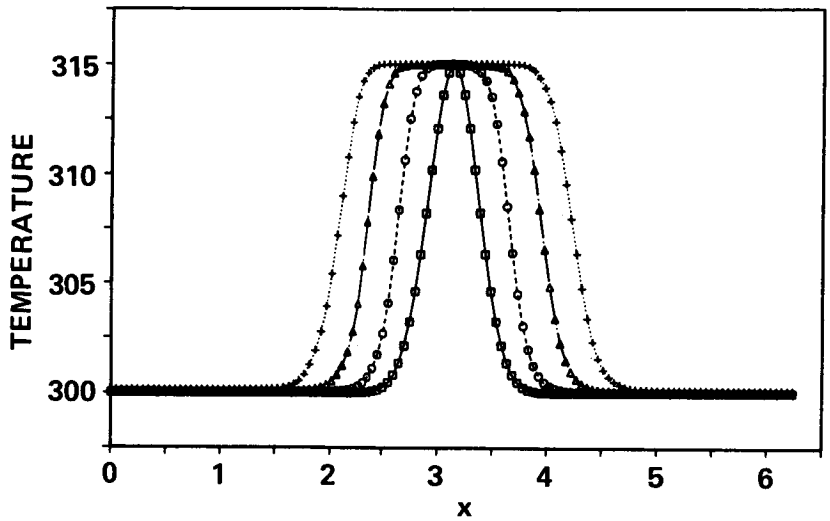

FIGURE 10. Mean turbulent temperature profiles at 200 step intervals.

Our plans to continue the work on this project include more analysis of the case we have presented here. In particular, we will examine scales and structures relating to the turbulent diffusion of the reactant mass fraction. We will also calculate the area of the wrinkled flame front and compare this to the turbulent flame speed. Further work in this area will include turbulent calculations with a mean strain-rate so that we can examine the effects of anisotropy on flame propagation.

REFERENCES

ABDEL-GAYAD, R. G. & BRADLEY, D. 1976 *Sixteenth Symposium (International) on Combustion*, The Combustion Institute.

CLAVIN, P. & WILLIAMS, F.A. 1979 Theory of premixed-flame propagation in large-scale turbulence. *J. Fluid Mech.* **90,** 589-604.

BRAY, K.N. 1980 Turbulent Flows with Premixed Reactants. *In Turbulent Reacting Flows, ed. P.A. Libby, F.A. Williams, Springer Verlag, Berlin.*

BRAY, K.N. & MOSS, J.B. 1977 *Acta Astron.*,**4.**

POPE, S.B. & ANAND, M.S. 1985 *Twentieth Symposium (International) on Combustion*, The Combustion Institute.

ROGALLO, R.S. 1981 Numerical Experiments in Homogeneous Turbulence. *NASA Technical Memorandum Number 81315.*

TABACZYNSKI, R.J., FERGUSON, C.R. & RADHAKRISHANAN, K. 1974 *SAE Paper Number 740191, SAE Trans.*,**83.**

WILLIAMS, F.A. 1985 *Combustion Theory*, Benjamin-Cummings, Reading, Mass.

WITZE, P.O. & MENDES-LOPES, J.M.C. 1986 *SAE Paper Number 861531.*

ZUR LOYE, A.O., & BRACCO F.V. 1987 *SAE Paper Number 870454.*